GEOPHYSICAL RESEARCH LETTERS, VOL. 19, NO. 7, PAGES 717-720, APRIL 3, 1992

3-D RADIATION PATTERN OF THE DRILLING BIT SOURCE IN FINELY STRATIFIED MEDIA

Jose M. Carcione and Philip M. Carrion

Osservatorio Geofisico Sperimentale, Trieste

Abstract: Seismic exploration industry is largely based on the concept of an impulsive point source whose radiation pattern in isotropic media is well-known. It is spherically isotropic in acoustic unbounded homogeneous media and directional in elastic media. A point source excitation in a simplified isotropic medium lend no credence what may happen in more realistic situations. In this paper, we present an analysis of the the radiation patterns for a vertical and a rotational loads distributed over a disk-shape surface placed in a finely stratified medium with a random distribution of elastic parameters. This complex source simulates the rotary drill tool used in boreholes. It is shown that the radiation patterns in these cases significantly differ from those computed for a point force in isotropic homogeneous media.

Introduction

Studies of radiation patterns are quite important from both theoretical and practical standpoints. This is due to the fact that the radiation pattern in realistic media significantly differs from the point-source radiation pattern corresponding to an isotropic homogeneous medium (e.g. Aki and Richards, 1980). Surprisingly, the geophysical literature is rather poor on this subject. This precludes a clear understanding of what might happen if a source with arbitrary load is placed in a realistic medium. Stam (1990) studied the seismic fields generated by a two-dimensional horizontal slab placed at the earth surface. Gangi (1987) carried out research towards the analysis of the radiation patterns of TBM sources (Tunnel-Boring Machines). He found that the radiation pattern of a TBM source is quite similar to one computed for a point source, except when the effects of the gripper pads are taken into account. Carrion and Sampaio (1991) developed a mathematical formalism for computing the radiation patterns of different seismic sources whose loads are distributed over the disks. All these authors, however, considered a simplified homogeneous elastic or acoustic media. In this letter, we investigate the radiation pattern of a drilling bit source assuming fine stratification. It is well-known that geological structures exhibit random behaviour in thin beds and thus can be succesfully modeled by fine layering. Geologically, this relates to such effects as compaction and sedimentary deposition. This makes quite necessary to carry out a rigorous analysis of the radiation patterns in finely stratified elastic media.

Paper number 92GL00543
0094-8534/92/92GL-00543$03.00

We use a full waveform pseudospectral scheme to compute the radiation patterns for vertical and torque loads distributed over a disk in a stratified elastic media with randomly distributed parameters. We found that the computed radiation patterns significantly differ from those corresponding to isotropic elastic media.

Numerical algorithm

The forward modeling code is based on the rapid expansion method (REM) as the time-integration algorithm, and the Fourier pseudospectral method for the computation of spatial derivatives (Kosloff et al., 1989). These techniques possess the spectral accuracy for band-limited signals not affected by temporal or spatial dispersion. An important advantage of our method compared to a conventional reflectivity approach is that it can accurately compute full waveforms also in the near field.

The model has randomly distributed elastic parameters: it consists of thin sandstone and limestone layers randomly entered in the model in equal proportions. At long wavelengths or low frequencies, the medium behaves as a nondispersive, smoothed, transversely isotropic material (Carcione et al., 1991). In fact, this is the case of downhole seismic sources in the presence of thin bed sedimentary formations. We use the Backus (1962) averaging technique to replace a layered medium by an effective transversely-isotropic medium.

The first source is taken in the form of a vertical force. Considering that the 3-D space is represented by the Cartesian coordinates x, y and z, the source vector is assumed to be directed along the z-axis:

$$\mathbf{f} = (0,\ 0,\ h(t)\delta(\mathbf{x} - \mathbf{x}_0)), \tag{1}$$

where $\mathbf{x}$ is the position vector, $\mathbf{x}_0$ is the location of the source, $h(t)$ is the source time function, and δ is the Dirac delta function. The second source is a pure torque whose cut-face is a disk with a Gaussian distribution stress function. For this source the vector potential is:

$$\mathbf{A} = A_z\hat{e}_z = \psi(\mathbf{x} - \mathbf{x}_0)h(t)\hat{e}_z \tag{2}$$

where $\psi(\mathbf{x} - \mathbf{x}_0)$ is a 3-D Gaussian function centered at $\mathbf{x}_0$. Therefore, the shear-source vector is given by:

$$\mathbf{f}^{(s)} = \nabla \times \mathbf{A} = \left(\frac{\partial A_z}{\partial y}, -\frac{\partial A_z}{\partial x}, 0\right). \tag{3}$$

The source configuration is displayed in Figure 1.

In a 3-D medium undergoing infinitesimal deformations, the equations of momentum conservation (e.g. Fung, 1965), including the vertical load and torque are expressed by

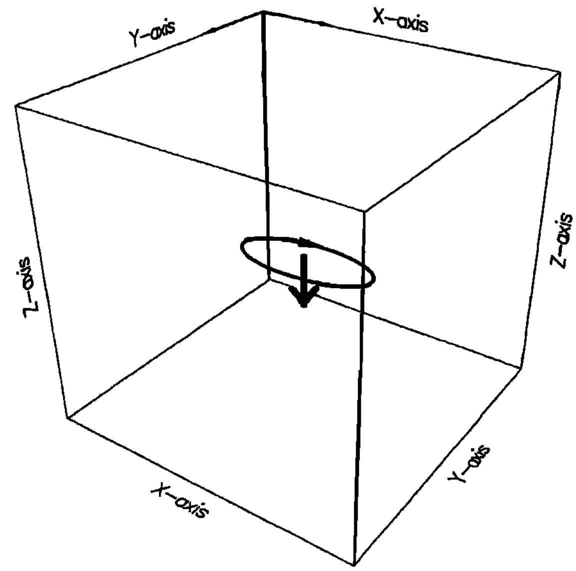

Fig. 1 Drilling bit source configuration. The source is a combination of the vertical force, and the torque load in the horizontal plane.

$$\rho \ddot{u}_x = \frac{\partial \sigma_{xx}}{\partial x} + \frac{\partial(\sigma_{xy} + A_z)}{\partial y} + \frac{\partial \sigma_{xz}}{\partial z},$$

$$\rho \ddot{u}_y = \frac{\partial(\sigma_{xy} - A_z)}{\partial x} + \frac{\partial \sigma_{yy}}{\partial y} + \frac{\partial \sigma_{yz}}{\partial z}, \tag{4}$$

$$\rho \ddot{u}_z = \frac{\partial \sigma_{xz}}{\partial x} + \frac{\partial \sigma_{yz}}{\partial y} + \frac{\partial \sigma_{zz}}{\partial z} + h(t)\delta(\mathbf{x} - \mathbf{x}_0),$$

where σ_{xx}, σ_{yy}, σ_{zz}, σ_{xy}, σ_{xz}, and σ_{yz} are the stress components; u_x, u_y and u_z are the displacement components, and ρ is the averaged density of the medium. The double dot above the displacements denotes second partial time derivatives (acceleration components).

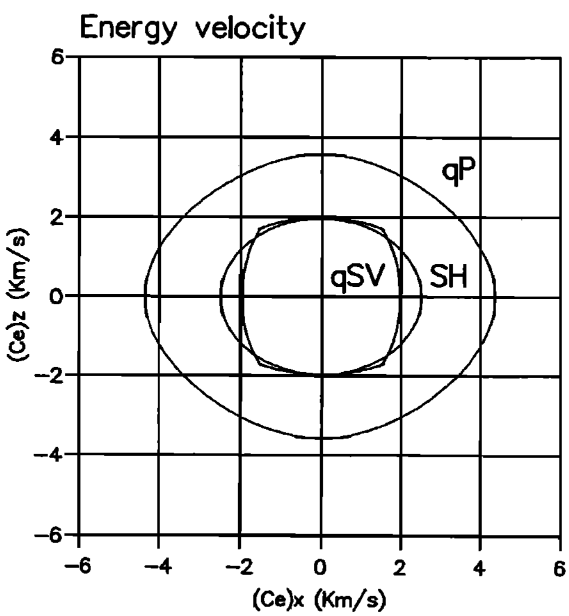

Fig. 2 Energy velocities in an effective transversely isotropic solid. The medium represents the long-wavelength equivalent of fine layering. Modes qP and qSV are coupled, while SH is pure.

The constitutive equation of a 3-D transversely-isotropic medium is given by

$$\begin{bmatrix} \sigma_{xx} \\ \sigma_{yy} \\ \sigma_{zz} \\ \sigma_{yz} \\ \sigma_{xz} \\ \sigma_{xy} \end{bmatrix} = \begin{bmatrix} c_{11} & c_{12} & c_{13} & 0 & 0 & 0 \\ & c_{11} & c_{13} & 0 & 0 & 0 \\ & & c_{33} & 0 & 0 & 0 \\ & & & c_{55} & 0 & 0 \\ & & & & c_{55} & 0 \\ & & & & & c_{66} \end{bmatrix} \begin{bmatrix} \varepsilon_{xx} \\ \varepsilon_{yy} \\ \varepsilon_{zz} \\ 2\varepsilon_{yz} \\ 2\varepsilon_{xz} \\ 2\varepsilon_{xy} \end{bmatrix}, \tag{5}$$

where

$$\varepsilon_{ij} = \frac{1}{2}\left(\frac{\partial u_i}{\partial x_j} + \frac{\partial u_j}{\partial x_i}\right), \qquad i,j = 1,2,3. \tag{6}$$

are the strain components, and $c_{IJ} = c_{JI}$, $I,J = 1,\ldots,6$ are the effective elastic moduli obtained from the Backus equations for media characterized by the Lame constants λ and μ.

$$c_{11} = \left\langle \frac{4\mu(\lambda+\mu)}{\lambda+2\mu} \right\rangle + \left\langle \frac{1}{\lambda+2\mu} \right\rangle^{-1} \left\langle \frac{\lambda}{\lambda+2\mu} \right\rangle^2,$$

$$c_{12} = \left\langle \frac{2\lambda\mu}{\lambda+2\mu} \right\rangle + \left\langle \frac{1}{\lambda+2\mu} \right\rangle^{-1} \left\langle \frac{\lambda}{\lambda+2\mu} \right\rangle^2,$$

$$c_{13} = \left\langle \frac{1}{\lambda+2\mu} \right\rangle^{-1} \left\langle \frac{\lambda}{\lambda+2\mu} \right\rangle,$$

$$c_{33} = \left\langle \frac{1}{\lambda+2\mu} \right\rangle^{-1}, \tag{7}$$

$$c_{55} = \left\langle \frac{1}{\mu} \right\rangle^{-1},$$

and

$$c_{66} = \langle \mu \rangle,$$

where $\langle\cdot\rangle$ denotes the thickness weighted average. The average density is simply $\rho = \langle\rho\rangle$.

Numerical results

In a typical seismic experiment, the sources and the receivers can be placed either at earth's surface or in boreholes. This indicates that knowledge of the radiation patterns of seismic sources will give a clear idea about the maximum or minimum of the detected seismic energy. Let us consider a source placed at some depth below the earth surface such that the effects of the free-surface can be neglected. We will place multicomponent geophones all around the source location.

The isotropic thin layers have the following values of compressional and shear velocities, and density, respectively: for sandstone, $V_P = 2950\ m/s$, $V_S = 1620\ m/s$ and $\rho = 2300\ Kg/m^3$, and for limestone, $V_P = 5440\ m/s$,

$V_S = 3040\ m/s$ and $\rho = 2700\ Kg/m^3$. The elastic moduli of the long-wavelength trasnversely-isotropic medium are, $c_{11} = 47.5\ GPa$, $c_{12} = 16.5\ GPa$, $c_{13} = 12.3\ GPa$, $c_{33} = 32\ GPa$, $c_{55} = 9.7\ GPa$ and $c_{66} = 15.5\ GPa$, and the average density is $\rho = 2500\ Kg/m^3$. The energy velocities $\mathbf{c}_e$ of the three propagating waves are represented in Figure 2. Modes qP and qSV are coupled, while SH is a pure mode. The wave fronts are the energy velocities multiplied by 1 s propagation time.

The numerical mesh has a size of $N_X = N_Y = N_Z = 99$, with a grid spacing of $D_X = D_Y = D_Z = 1.5\ m$. The source time function is given by a Ricker wavelet,

$$h(t) = e^{\frac{1}{2}f_0^2(t-t_0)^2} \cos \pi f_0(t - t_0), \tag{8}$$

where $t_0 = 6\ ms$ and $f_0 = 500\ Hz$, i.e., a central frequency of $250\ Hz$. This source function activates the drill bit tool approximately $12\ ms$.

The following figures are snapshots of the wavefield at $18\ ms$ in the vertical xz-plane intersecting the source location $\mathbf{x}_0$. Figure 3 depicts the z-component of the displacement, where only the vertical force contributes. One can observe that the compressional energy (qP wave) is confined within small look angles around the vertical axis. This means that the maximum of compressional energy will be detected by the geophones located at a horizontal surface. It is interesting to notice that the qSV waves are characterized by unusually high amplitudes. These arrivals will be detected at the opposite borehole with maximum at the cut-face plane of the source. It is also interesting to see that the recorded phase surfaces exhibit an elliptic-type shape.

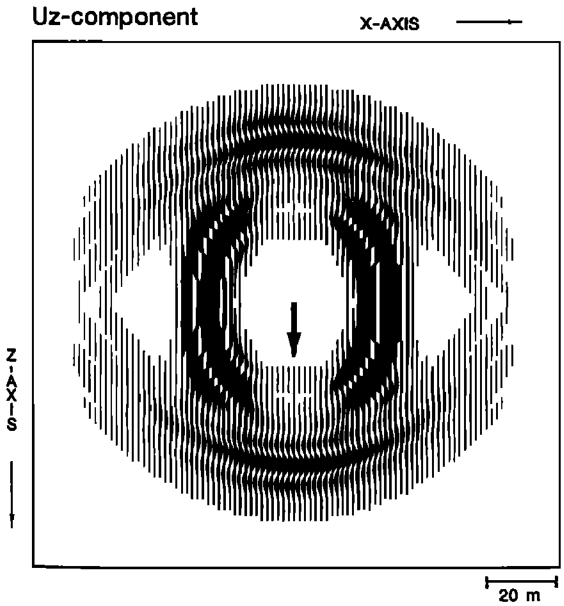

Fig. 3 Vertical component of the displacement, where only the vertical force contributes. Note that compressional energy is confined within small look angles around the z-axis, and that cusps of the qSV mode are characterized by high amplitudes. The recording plane is normal to the y-axis.

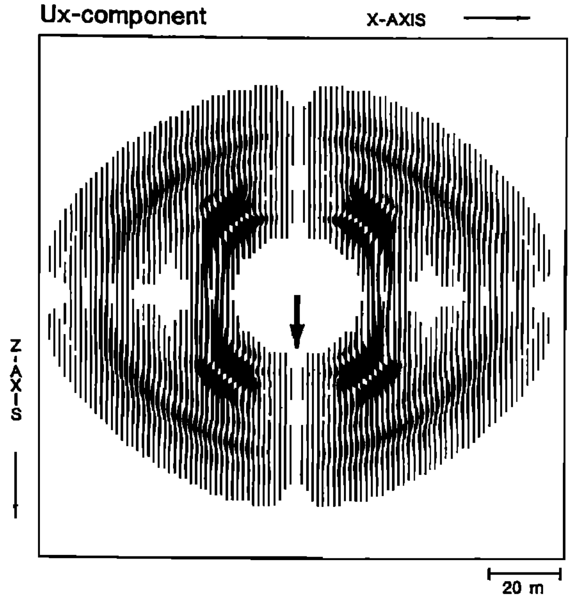

Fig. 4 Horizontal component (x-directed) of the displacement. As in Figure 3, the energy comes solely from the vertical force. Most of this energy is concentrated at approximately $\pi/4$ from the vertical axis. The recording plane is normal to the y-axis.

Figure 4 depicts the recordings obtained by a horizontally directed (x-direction) geophones that surround the source location. As before, only the vertical force contributes to this component. One can observe that in this case the high energy cusps of shear waves (qSV) occur. These cusps are absent on the radiation pattern displays related to a homogeneous isotropic medium. It is shown that in the neighborhood of the vertical axis for small look angles the x-directed geophones will not record any significant energies. The same is true for the cut-face plane. The most energy is concentrated near the bisect of the Figure 4, and thus not much energy will be recorded in the opposite borehole.

Due to symmetry arguments, the u_x wave fronts should show antisymmetric behaviour across $x = 0$ and $z = 0$, and the u_z wave fronts show symmetric behaviour across the same lines. The effects can be visualized for both components across $z = 0$, but due to the nature of the display, these are not evident across $x = 0$. However, a careful analysis reveals that equidistant points at both sides of the line $x = 0$ for the x-component have the same amplitude but opposite sign (antisymmetry). The same analysis show that the z -component is symmetric across $x = 0$.

Figure 5 illustrates the y -component of the displacement of the torque source in the xz-vertical plane. The energy comes from the torque force, other components of this source vanish. It corresponds to pure SH waves with elliptic phase surface. This has an important impact on interpretation of complex seismic sources. Suppose a geophone is located at some distance from the vertical axis (non-zero offset recording) and detects the y -component of the displacement field. This means that at this moment the complex source acts as a pure torque. Our result also shows that the pilot recording would not be recorded at small look angles where the energy of shear waves is minimal.

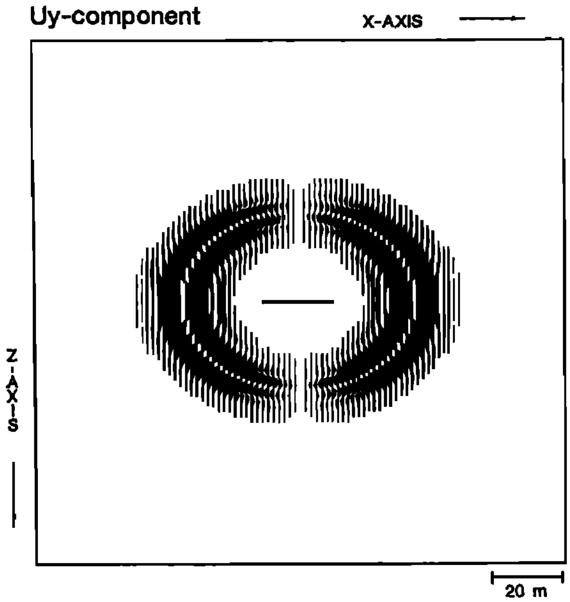

Fig. 5 Horizontal component (y-directed) of the displacement. As is expected, pure shear arrivals from the torque force are recorded by y-directed geophones.

Conclusions

Our results demonstrate that the radiation pattern of seismic sources placed in a finely stratified medium with vertical random distribution of elastic parameters can be significantly different from those computed for isotropic homogeneous media. Since real situations can not be described even approximately by homogeneous isotropic media, the effects related to fine layering should be taken into account. An important result of this letter is that one can analyze seismic events using a multicomponent recording to interprete complex seismic sources. In particular, if a source is a combination of the vertical and a torque loads like the drilling bit, the SH-component of the wavefield indicates at which instances the source would act as a pure torque.

References

Aki, K. and Richards, P. G., Quantitative Seismology, theory and methods, Vol. 1, 557 pp., W. H. Freeman and Company, 1980.

Backus, G. E., Long-wave elastic anisotropy produced by horizontal layering, J. Geophys. Res., 67, 4427-4440, 1962.

Carcione, J. M., Kosloff, D., and Behle, A., Long-wave anisotropy in stratified media: A numerical test, Geophysics, 56, 245-254, 1991.

Carrion, P. M., and Sampaio, E., Radiation pattern of seismic sources via disk-source analysis, Proceedings of the II SBGF Meeting, 1, 861, 1991.

Fung, Y. C., Foundations of solid mechanics, 525 pp., Prentice Hall Inc, 1965.

Gangi, A. F., A theoretical study of the radiation patterns of a tunnel-boring machine (infinite medium), Rep. GL-87-20, 114 pp., Texas A&M University, 1987.

Kosloff, D. M., Carcione, J. M., Rommel, B., and Behle, A., Three-dimensional wave propagation simulation in elastic-anisotropic media (expanded abstract), Society of Exploration Geophysicists, 59th annual meeting, 2, 1016, 1989.

Stam, H. J., The two-dimensional elastodynamic distributed surface load problem, Geophysics, 55, 1047, 1990.

J. M. Carcione and P. M. Carrion, Osservatorio Geofisico Sperimentale, P.O. Box 2011, 34016 Trieste, Italy.

(Received: December 17, 1991;
(Accepted: January 28, 1992.)